







Article

On Multiple-Type Wave Solutions for the Nonlinear Coupled Time-Fractional Schrödinger Model

Pshtiwan Othman Mohammed ^{1,2,*} , Ravi P. Agarwal ³ , Iver Brevik ⁴ , Mohamed Abdelwahed ⁵ ,
Artion Kashuri ⁶  and Majeed A. Youisif ⁷ ¹ Department of Mathematics, College of Education, University of Sulaimani, Sulaymaniyah 46001, Iraq² Research and Development Center, University of Sulaimani, Sulaymaniyah 46001, Iraq³ Department of Mathematics and Systems Engineering, Florida Institute of Technology, Melbourne, FL 32901, USA⁴ Department of Energy and Process Engineering, Norwegian University of Science and Technology, N-7491 Trondheim, Norway; iver.h.brevik@ntnu.no⁵ Department of Mathematics, College of Science, King Saud University, P.O. Box 2455, Riyadh 11451, Saudi Arabia⁶ Department of Mathematical Engineering, Polytechnic University of Tirana, 1001 Tirana, Albania⁷ Department of Mathematics, College of Education, University of Zakho, Zakho 42002, Iraq; majeed.yousif@uoz.edu.krd

* Correspondence: pshtiwanasangawi@gmail.com

Abstract: Recently, nonlinear fractional models have become increasingly important for describing phenomena occurring in science and engineering fields, especially those including symmetric kernels. In the current article, we examine two reliable methods for solving fractional coupled nonlinear Schrödinger models. These methods are known as the Sardar-subequation technique (SSET) and the improved generalized tanh-function technique (IGTHFT). Numerous novel soliton solutions are computed using different formats, such as periodic, bell-shaped, dark, and combination single bright along with kink, periodic, and single soliton solutions. Additionally, single solitary wave, multi-wave, and periodic kink combined solutions are evaluated. The behavioral traits of the retrieved solutions are illustrated by certain distinctive two-dimensional, three-dimensional, and contour graphs. The results are encouraging, since they show that the suggested methods are trustworthy, consistent, and efficient in finding accurate solutions to the various challenging nonlinear problems that have recently surfaced in applied sciences, engineering, and nonlinear optics.

Keywords: multiple-wave solutions; coupled nonlinear fractional-order Schrödinger model; Sardar-subequation technique; improved generalized tanh-function technique

MSC: 26A48; 26A51; 33B10; 39A12; 39B62



check for updates

Citation: Mohammed, P.O.; Agarwal, R.P.; Brevik, I.; Abdelwahed, M.; Kashuri, A.; Youisif, M.A. On Multiple-Type Wave Solutions for the Nonlinear Coupled Time-Fractional Schrödinger Model. *Symmetry* **2024**, *16*, 553. <https://doi.org/10.3390/sym16050553>

Academic Editor: Pasquale Candito

Received: 26 March 2024

Revised: 24 April 2024

Accepted: 29 April 2024

Published: 3 May 2024



Copyright: © 2024 by the authors. Licensee MDPI, Basel, Switzerland. This article is an open access article distributed under the terms and conditions of the Creative Commons Attribution (CC BY) license (<https://creativecommons.org/licenses/by/4.0/>).

1. Introduction

Nonlinear partial differential equations (NLPDEs) find applications in a myriad of scientific and engineering fields, including atmospheric science, climate modeling, combustion dynamics, population dynamics, pattern formation, material science, seismic wave propagation, plasma physics, astrophysics, and biological systems modeling. These equations are employed to model complex phenomena such as turbulent flows, chemical reactions, wave interactions, and nonlinear wave propagation in various mediums. They are essential for understanding and predicting the behavior of complex systems in both natural and engineered environments. However, due to the inherent complexity of NLPDEs [1–6], finding exact solutions using a single technique is often challenging. To address this, several reliable methods have been proposed, for instance, the modified $\exp(-\phi(\omega))$ -expansion function [7,8], the sin-Gordon-expansion [9], the $\frac{G'}{G^2}$ -expansion function [10], the

first integral approach [11], and the Hirota bilinear approach [12,13]. Additionally, various strategies have been explored for deriving lump solutions [14]. Optical solitons, renowned for their capacity to transmit waves over extensive distances without dispersion, represent a significant research domain within optics and optoelectronics [15]. These solitons have revolutionized the telecom industry, leading to advancements in high-speed communication systems [16–21]. As a result, fractional-order NLPDEs have garnered attention in recent studies, particularly in optics and other applied sciences, owing to their potential applications in modeling highly nonlinear phenomena [22–24]. Fractional-order derivatives offer advantages over integer derivatives, providing more accurate mathematical and physical models for various technical issues [25–27]. Consequently, fractional NLSE models have become essential for understanding soliton dynamics in optical fibers, with various solution schemes developed over the past two decades [28–39]. The motivation behind this study stems from the growing need to address complex nonlinear phenomena across diverse scientific disciplines, particularly in optics and applied sciences. The main goal is to employ advanced techniques to solve fractionally coupled nonlinear Schrödinger models and extract multiple-wave solutions. The Sardar-subequation technique (SSET) is a powerful method employed in the realm of solving nonlinear differential equations. With its efficacy demonstrated across various disciplines, numerous researchers have leveraged SSET to tackle complex problems and unveil novel solutions. For instance, Ref. [40] utilized SSET to derive new solitary wave solutions for the (3+1)-dimensional Wazwaz–Benjamin–Bona–Mahony equations, showcasing its effectiveness in handling intricate systems. Similarly, Ref. [41] employed SSET to explore new wave solutions for a nonlinear Landau–Ginzburg–Higgs equation, revealing diverse types of solitons such as bright and dark solitons, singular periodic solitons, and hybrid solitons. Moreover, Ref. [42] extended the application of SSET to the (4+1)-dimensional fractional-order Fokas equation, demonstrating its capability in generating various soliton solutions. Ref. [43] utilized SSET to obtain exact wave solutions for a complex three-coupled Maccari’s system, further highlighting its versatility. Additionally, research in [44] has integrated SSET with conformable derivatives to investigate solitary solutions for the conformable fractional Klein–Gordon equation with high-order non-linearity. Overall, the Sardar-subequation technique (SSET) stands as a valuable tool in the arsenal of techniques for solving nonlinear differential equations, offering insights into a wide range of physical phenomena and mathematical models. The generalized tanh-function technique has emerged as a versatile method for solving a variety of fractional differential equations, offering insights into the dynamics of complex systems. Researchers have applied the GTHFT to address significant equations across different domains. For instance, Ref. [45] utilized the GTHFT to tackle the time-fractional Sharma–Tasso–Olver equation and the space-time fractional Kowerteg–de Vries–Burgers equations, showcasing its efficacy in handling both time- and space-fractional derivatives. Similarly, Ref. [46] employed the tanh-function technique to solve the time-fractional modified Liouville and mRLW equations, unraveling the dynamical behavior of traveling wave solutions. Ref. [47] further advanced the method, refining and modifying the tanh-function approach to uncover exact traveling wave solutions for a family of 3D fractional Wazwaz–Benjamin–Bona–Mahony equations, demonstrating its adaptability and precision. Moreover, Ref. [48] extended the tanh function approach to address nonlinear time-fractional Klein–Gordon and Sine–Gordon equations, revealing new traveling wave solutions. Through these applications, the generalized tanh-function technique continues to prove its utility in unraveling the intricate dynamics of fractional differential equations, paving the way for deeper understanding and analysis in various scientific disciplines. The novel aspect of this study is the application of both SSET and IGTHFT to derive a variety of soliton solutions. These solutions encompass periodic, bell-shaped, dark, and composite single bright solitons, along with kink, periodic, and single soliton solutions. Additionally, the exploration of single solitary wave, multi-wave, and periodic kink combined solutions adds further depth to the analysis. Through the illustration of distinct behavioral traits using two-dimensional, three-dimensional, and contour graphs, this study contributes

valuable insights into the accurate and efficient solutions to challenging nonlinear problems encountered in applied sciences, engineering, and nonlinear optics.

Consider the coupled nonlinear fractional-order Schrödinger equations

$$\begin{aligned} iD_t^\delta \Xi_1 + D_x^{2\gamma} \Xi_1 + \alpha \left(|\Xi_1|^2 + \beta |\Xi_2|^2 \right) \Xi_1 &= 0, \\ iD_t^\delta \Xi_2 + D_x^{2\gamma} \Xi_2 + \alpha \left(|\Xi_1|^2 + \beta |\Xi_2|^2 \right) \Xi_2 &= 0, \end{aligned} \quad (1)$$

where $x \in [-\infty, \infty]$, $t > 0$, and the behavior of polarized waves within nonlinear fiber optics, with constraints $0 < \delta, \gamma \leq 1$. The functions $\Xi_1(x, t)$ and $\Xi_2(x, t)$ intricately depict the dynamic range of these waves in relation to t and x . Parameters α and β are real and non-zero integers. Our study employs two distinct methodologies: enhancements to the generalized tanh-function technique and the Sardar-subequation technique. These methodologies are applied under various conditions to deduce soliton and solitary wave solutions for the given model.

The paper is organized as follows. Section 2 covers the basics of conformable fractional derivatives. Section 3 introduces the SSET and IGTHFT techniques. Results and discussions are provided in Section 4, while concluding remarks are presented in Section 5.

2. Conformable Derivative

Fractional-order derivatives have attracted significant attention from researchers due to their broad applications across diverse scientific fields. Various fractional derivative operators, including the Caputo–Fabrizio, Caputo, and Riemann–Liouville fractional derivatives, have been developed to provide innovative approaches for modeling intricate phenomena and accurately capturing memory effects and non-local behavior. These operators play crucial roles in classical dynamics, banking, discrete mathematics, microbiology, plastics research, elasticity studies, and numerous other scientific domains. Their capability to describe systems with fractional dimensions and represent non-local effects makes them indispensable tools for comprehending and analyzing a wide range of physical processes. Moreover, the conformable derivative, introduced by Khalil et al. in 2014 [49], stands out as a promising addition to fractional calculus, offering simplified and efficient solutions for various mathematical and scientific challenges.

Definition 1. Given a function $p : [0, \infty] \rightarrow \mathbb{R}$, the conformable fractional derivative of p of order δ is defined by [49]

$$T_\delta(p(t)) = \lim_{\omega \rightarrow 0} \frac{p(t + \omega t^{1-\delta}) - p(t)}{\omega}, \quad 0 < \delta \leq 1. \quad (2)$$

Definition 2. Let $\delta \in (n, n + 1]$ and p be n -differentiable at t , where $t > 0$. Then the conformable fractional derivative for p of order δ is defined as [49]

$$T_\delta(p)(t) = \lim_{\omega \rightarrow 0} \frac{p^{([\delta]-1)}(t + \omega t^{([\delta]-\delta)}) - p^{([\delta]-1)}(t)}{\omega}, \quad (3)$$

where $[\delta]$ is the smallest integer greater than or equal to δ .

Properties 1. Some Properties of Conformable Fractional Derivative [49]

Let $\delta \in (0, 1]$, $a \in \mathbb{R}$ and Θ, Σ are δ -differentiable at point $t > 0$, then:

1. $T_\delta(a_1\Theta + a_2\Sigma) = a_1T_\delta(\Theta) + a_2T_\delta(\Sigma)$, for all $a_1, a_2 \in \mathbb{R}$.
2. $T_\delta(t^a) = at^{a-\delta}$, for all $a \in \mathbb{R}$.
3. $T_\delta(\Theta(t)) = 0$, if $\Theta(t)$ is constant function.
4. $T_\delta(\Theta)(t) = t^{1-\delta} \frac{d\Theta}{dt}(t)$.
5. $T_\delta(\sin at) = at^{1-\delta} \cos at$.

6. $T_\delta(\cos at) = -at^{1-\delta} \sin at.$
7. $T_\delta(e^{at}) = at^{1-\delta} e^{at}.$

Theorem 1. Assume $\Theta, \Sigma : (0, \infty) \rightarrow \mathbb{Q}$, $0 < \delta \leq 1$ are two differentiable functions, then the following chain rule holds:

$$T_\delta(\Theta \circ \Sigma)(t) = t^{(1-\delta)} (\Sigma(t))^{(\delta-2)} \Sigma'(t) T_\delta(\Theta(t)) |_{t=\Theta(t)}. \quad (4)$$

3. Analytical Investigation

The main aim of this section is to gather a multitude of solutions for the models presented in this study. This is accomplished by substituting the following complex wave transformations for solving Equation (1):

$$\Xi_1(x, t) = \varphi_1(\xi) e^{i\omega}, \quad (5)$$

$$\Xi_2(x, t) = \varphi_2(\xi) e^{i\omega}, \quad (6)$$

and

$$\xi = n \left(\frac{x^\gamma}{\gamma} - b \frac{t^\delta}{\delta} \right), \quad \omega = -\sigma \frac{x^\gamma}{\gamma} + \omega \frac{t^\delta}{\delta} + \vartheta_0,$$

where n, σ and ω represent real constants, while ϑ_0 denotes an arbitrary constant. To obtain the real and imaginary parts of Equation (1), the complex wave transformations (5) and (6) are substituted into (1).

$$\begin{aligned} n^2 \varphi_1'' + \alpha \varphi_1^3 + \alpha \beta \varphi_2^2 \varphi_1 - (\sigma^2 + \omega) \varphi_1 &= 0, \\ n^2 \varphi_2'' + \alpha \varphi_2^3 + \alpha \beta \varphi_1^2 \varphi_2 - (\sigma^2 + \omega) \varphi_2 &= 0, \end{aligned} \quad (7)$$

and

$$d = -2\sigma, \quad (8)$$

$$\varphi_2 = f \varphi_1. \quad (9)$$

Then (7), becomes

$$n^2 \varphi_1'' + (\alpha + \alpha \beta f^2) \varphi_1^3 - (\sigma^2 + \omega) \varphi_1 = 0. \quad (10)$$

3.1. Application of the SSET

Consider the solution of Equation (10), as

$$\varphi_1(\xi) = \sum_{l=0}^N \Omega_l \Phi^l(\xi). \quad (11)$$

In this context, the coefficients required for solving are denoted by $\Omega_l, l = 0, 1, 2, \dots, N$, and $\Phi(\xi)$ satisfies the specified ordinary differential equation.

$$\Phi'(\xi) = \sqrt{\rho + h\Phi^2(\xi) + \Phi^4(\xi)}, \quad (12)$$

where h and ρ stand for real constants awaiting evaluation, while the value of N is ascertained by applying the homogeneous balancing principle. Balancing the terms φ_1'' and φ_1^3 of Equation (10), we find $N = 1$. Thus, Equation (11) is converted into:

$$\varphi_1(\xi) = \Omega_0 + \Omega_1 \Phi(\xi). \quad (13)$$

To proceed, differentiate Equation (13) twice and substitute it into Equation (10). This process yields a set of algebraic polynomials. The solutions to these polynomials, obtained using Mathematica software, are as follows:

$$\left\{ \sigma \rightarrow -\sqrt{hn^2 - \omega}, \Omega_0 \rightarrow 0, \Omega_1 \rightarrow -\frac{\sqrt{2}n}{\sqrt{-\alpha(\beta f^2 + 1)}} \right\}. \quad (14)$$

Using the solution set, we derive the following solutions.

Case-1 If $h, \rho < 0$, we have

$$\varphi_{1,1}(x, t) = -\frac{\sqrt{6}n\sqrt{-\frac{amn}{g}} \sec\left(\sqrt{3}\sqrt{-\frac{a}{g}}\left(\frac{nx^\gamma}{\gamma} - \frac{bt^\delta}{\delta}\right)\right)}{\sqrt{-\alpha(\beta f^2 + 1)}}, \quad (15)$$

or

$$\varphi_{1,2}(x, t) = -\frac{\sqrt{2}n\sqrt{-hmn} \csc\left(\sqrt{-hn}\left(\frac{x^\gamma}{\gamma} - \frac{bt^\delta}{\delta}\right)\right)}{\sqrt{-\alpha(\beta f^2 + 1)}}. \quad (16)$$

Case-2

If $h > 0$ and $\rho = 0$, we obtain

$$\varphi_{1,3}(x, t) = -\frac{\sqrt{2}n\sqrt{-hmn} \operatorname{sech}\left(\sqrt{hn}\left(\frac{x^\gamma}{\gamma} - \frac{bt^\delta}{\delta}\right)\right)}{\sqrt{-\alpha(\beta f^2 + 1)}}, \quad (17)$$

or

$$\varphi_{1,4}(x, t) = -\frac{\sqrt{2}n\sqrt{-hmn} \operatorname{csch}\left(\sqrt{hn}\left(\frac{x^\gamma}{\gamma} - \frac{bt^\delta}{\delta}\right)\right)}{\sqrt{-\alpha(\beta f^2 + 1)}}. \quad (18)$$

Case-3

If $h < 0$ and $\rho = \frac{h^2}{4d}$, we obtain

$$\varphi_{1,5}(x, t) = -\frac{\sqrt{-hn} \tanh\left(\frac{\sqrt{-hn}\left(\frac{x^\gamma}{\gamma} - \frac{bt^\delta}{\delta}\right)}{\sqrt{2}}\right)}{\sqrt{-\alpha(\beta f^2 + 1)}}, \quad (19)$$

or

$$\varphi_{1,6}(x, t) = -\frac{\sqrt{-hn} \coth\left(\frac{\sqrt{-hn}\left(\frac{x^\gamma}{\gamma} - \frac{bt^\delta}{\delta}\right)}{\sqrt{2}}\right)}{\sqrt{-\alpha(\beta f^2 + 1)}}, \quad (20)$$

or

$$\varphi_{1,7}(x, t) = -\frac{\sqrt{2}n\left(\frac{\sqrt{-h} \tanh\left(\sqrt{2}\sqrt{-hn}\left(\frac{x^\gamma}{\gamma} - \frac{bt^\delta}{\delta}\right)\right)}{\sqrt{2}} + i\sqrt{mn} \operatorname{sech}\left(\sqrt{2}\sqrt{-hn}\left(\frac{x^\gamma}{\gamma} - \frac{bt^\delta}{\delta}\right)\right)\right)}{\sqrt{-\alpha(\beta f^2 + 1)}}, \quad (21)$$

or

$$\varphi_{1,8}(x, t) = -\frac{\sqrt{2}n\left(\frac{\sqrt{-h} \coth\left(\sqrt{2}\sqrt{-hn}\left(\frac{x^\gamma}{\gamma} - \frac{bt^\delta}{\delta}\right)\right)}{\sqrt{2}} + i\sqrt{mn} \operatorname{csch}\left(\sqrt{2}\sqrt{-hn}\left(\frac{x^\gamma}{\gamma} - \frac{bt^\delta}{\delta}\right)\right)\right)}{\sqrt{-\alpha(\beta f^2 + 1)}}, \quad (22)$$

or

$$\varphi_{1,9}(x, t) = - \frac{\sqrt{2n} \left(\frac{\sqrt{-b} \tanh \left(\frac{\sqrt{-bn} \left(\frac{x^\gamma}{\gamma} - \frac{bt^\delta}{\delta} \right)}{2\sqrt{2}} \right)}{2\sqrt{2}} + i\sqrt{mn} \coth \left(\frac{\sqrt{-bn} \left(\frac{x^\gamma}{\gamma} - \frac{bt^\delta}{\delta} \right)}{2\sqrt{2}} \right) \right)}{\sqrt{-\alpha(\beta f^2 + 1)}}. \quad (23)$$

Case-4

If $h > 0$ and $\rho = \frac{h^2}{4d}$, we have

$$\varphi_{1,10}(x, t) = - \frac{\sqrt{-bn} \tan \left(\frac{\sqrt{hn} \left(\frac{x^\gamma}{\gamma} - \frac{bt^\delta}{\delta} \right)}{\sqrt{2}} \right)}{\sqrt{-\alpha(\beta f^2 + 1)}}, \quad (24)$$

or

$$\varphi_{1,11}(x, t) = - \frac{\sqrt{-bn} \cot \left(\frac{\sqrt{hn} \left(\frac{x^\gamma}{\gamma} - \frac{bt^\delta}{\delta} \right)}{\sqrt{2}} \right)}{\sqrt{-\alpha(\beta f^2 + 1)}}, \quad (25)$$

or

$$\varphi_{1,12}(x, t) = - \frac{\sqrt{-bn} \left(\tan \left(\sqrt{2}\sqrt{hn} \left(\frac{x^\gamma}{\gamma} - \frac{bt^\delta}{\delta} \right) \right) + \sec \left(\sqrt{2}\sqrt{hn} \left(\frac{x^\gamma}{\gamma} - \frac{bt^\delta}{\delta} \right) \right) \right)}{\sqrt{-\alpha(\beta f^2 + 1)}}, \quad (26)$$

or

$$\varphi_{1,13}(x, t) = - \frac{\sqrt{-bn} \left(\cot \left(\sqrt{2}\sqrt{hn} \left(\frac{x^\gamma}{\gamma} - \frac{bt^\delta}{\delta} \right) \right) + \csc \left(\sqrt{2}\sqrt{hn} \left(\frac{x^\gamma}{\gamma} - \frac{bt^\delta}{\delta} \right) \right) \right)}{\sqrt{-\alpha(\beta f^2 + 1)}}, \quad (27)$$

or

$$\varphi_{1,14}(x, t) = - \frac{\sqrt{hn} \left(\tan \left(\frac{\sqrt{hn} \left(\frac{x^\gamma}{\gamma} - \frac{bt^\delta}{\delta} \right)}{2\sqrt{2}} \right) + \cot \left(\frac{\sqrt{hn} \left(\frac{x^\gamma}{\gamma} - \frac{bt^\delta}{\delta} \right)}{2\sqrt{2}} \right) \right)}{2\sqrt{-\alpha(\beta f^2 + 1)}}. \quad (28)$$

3.2. Application of the IGTHFT

In this context, the solution of Equation (10) is as follows:

$$\varphi_1(\xi) = p_0 + \sum_{r=1}^N p_r \Theta^r(\xi) + \sum_{r=1}^N \frac{q_r}{\Theta^r(\xi)}, \quad (29)$$

where q_r and p_r , with $r = 0, 1, 2, \dots, N$, denote the coefficients essential for the solution, while $\Theta(\xi)$ adheres to the prescribed Riccati differential equation.

$$\Theta'(\xi) = \Theta^2(\xi) + v, \quad (30)$$

where v represents a constant that determines the value of N . We utilize the homogeneous balancing principle to determine N . Balancing the terms φ_1'' and φ_1^3 of Equation (10), we find $N = 1$. Thus, Equation (11) is transformed into

$$\varphi_1(\xi) = p_0 + p_1 \Theta(\xi) + \frac{q_1}{\Theta(\xi)}. \quad (31)$$

To proceed, differentiate Equation (31) twice and substitute the desired values into Equation (10). This process yields a set of algebraic polynomials. The outcomes derived from solving these polynomials with Mathematica software are as follows:

Set-1

$$\left\{ p_0 \rightarrow 0, p_1 \rightarrow -\frac{\sqrt{2}n}{\sqrt{-\alpha(\beta f^2 + 1)}}, q_1 \rightarrow -\frac{\sqrt{2}nv}{\sqrt{-\alpha(\beta f^2 + 1)}}, \omega \rightarrow -4n^2v - \sigma^2 \right\}. \quad (32)$$

According to the solution set, we have the following solutions.

Case-1

If $\mu < 0$, we obtain

$$\varphi_{2,1}(x, t) = \frac{2\sqrt{3}nv \coth\left(\frac{\sqrt{-\mu n}\left(\frac{x^\gamma}{\gamma} - \frac{bt^\delta}{\delta}\right)}{\sqrt{6}}\right)}{\sqrt{-\mu}\sqrt{-\alpha(\beta f^2 + 1)}} + \frac{\sqrt{-\mu n} \tanh\left(\frac{\sqrt{-\mu n}\left(\frac{x^\gamma}{\gamma} - \frac{bt^\delta}{\delta}\right)}{\sqrt{6}}\right)}{\sqrt{3}\sqrt{-\alpha(\beta f^2 + 1)}}, \quad (33)$$

or

$$\varphi_{2,2}(x, t) = \frac{2\sqrt{3}nv \tanh\left(\frac{\sqrt{-\mu n}\left(\frac{x^\gamma}{\gamma} - \frac{bt^\delta}{\delta}\right)}{\sqrt{6}}\right)}{\sqrt{-\mu}\sqrt{-\alpha(\beta f^2 + 1)}} + \frac{\sqrt{-\mu n} \coth\left(\frac{\sqrt{-\mu n}\left(\frac{x^\gamma}{\gamma} - \frac{bt^\delta}{\delta}\right)}{\sqrt{6}}\right)}{\sqrt{3}\sqrt{-\alpha(\beta f^2 + 1)}}. \quad (34)$$

Case-2

If $\mu = 0$, we obtain

$$\varphi_{2,3}(x, t) = \frac{2\sqrt{3}}{\sqrt{-\alpha(\beta f^2 + 1)}\left(\frac{x^\gamma}{\gamma} - \frac{bt^\delta}{\delta}\right)} - \frac{n^2v\left(\frac{x^\gamma}{\gamma} - \frac{bt^\delta}{\delta}\right)}{\sqrt{3}\sqrt{-\alpha(\beta f^2 + 1)}}. \quad (35)$$

Case-3

If $\mu > 0$, we have

$$\varphi_{2,4}(x, t) = \frac{2\sqrt{3}nv \coth\left(\frac{\sqrt{\mu n}\left(\frac{x^\gamma}{\gamma} - \frac{bt^\delta}{\delta}\right)}{\sqrt{6}}\right)}{\sqrt{\mu}\sqrt{-\alpha(\beta f^2 + 1)}} + \frac{\sqrt{\mu n} \tanh\left(\frac{\sqrt{\mu n}\left(\frac{x^\gamma}{\gamma} - \frac{bt^\delta}{\delta}\right)}{\sqrt{6}}\right)}{\sqrt{3}\sqrt{-\alpha(\beta f^2 + 1)}}, \quad (36)$$

or

$$\varphi_{2,5}(x, t) = \frac{2\sqrt{3}nv \tanh\left(\frac{\sqrt{\mu n}\left(\frac{x^\gamma}{\gamma} - \frac{bt^\delta}{\delta}\right)}{\sqrt{6}}\right)}{\sqrt{\mu}\sqrt{-\alpha(\beta f^2 + 1)}} + \frac{\sqrt{\mu n} \coth\left(\frac{\sqrt{\mu n}\left(\frac{x^\gamma}{\gamma} - \frac{bt^\delta}{\delta}\right)}{\sqrt{6}}\right)}{\sqrt{3}\sqrt{-\alpha(\beta f^2 + 1)}}. \quad (37)$$

Set-2

$$\left\{ p_0 \rightarrow 0, p_1 \rightarrow \frac{\sqrt{2}n}{\sqrt{-\alpha(\beta f^2 + 1)}}, q_1 \rightarrow \frac{\sqrt{2}nv}{\sqrt{-\alpha(\beta f^2 + 1)}}, \omega \rightarrow -4n^2v - \sigma^2 \right\}. \quad (38)$$

According to the solution set, we obtain the following solutions.

Case-1

If $\mu < 0$, we obtain

$$\varphi_{2,6}(x, t) = -\frac{2\sqrt{3}nv \coth\left(\frac{\sqrt{-\mu}n\left(\frac{x^\gamma}{\gamma} - \frac{bt^\delta}{\delta}\right)}{\sqrt{6}}\right)}{\sqrt{-\mu}\sqrt{-\alpha(\beta f^2 + 1)}} - \frac{\sqrt{-\mu}n \tanh\left(\frac{\sqrt{-\mu}n\left(\frac{x^\gamma}{\gamma} - \frac{bt^\delta}{\delta}\right)}{\sqrt{6}}\right)}{\sqrt{3}\sqrt{-\alpha(\beta f^2 + 1)}}, \quad (39)$$

or

$$\varphi_{2,7}(x, t) = -\frac{2\sqrt{3}nv \tanh\left(\frac{\sqrt{-\mu}n\left(\frac{x^\gamma}{\gamma} - \frac{bt^\delta}{\delta}\right)}{\sqrt{6}}\right)}{\sqrt{-\mu}\sqrt{-\alpha(\beta f^2 + 1)}} - \frac{\sqrt{-\mu}n \coth\left(\frac{\sqrt{-\mu}n\left(\frac{x^\gamma}{\gamma} - \frac{bt^\delta}{\delta}\right)}{\sqrt{6}}\right)}{\sqrt{3}\sqrt{-\alpha(\beta f^2 + 1)}}. \quad (40)$$

Case-2

If $\mu = 0$, we have

$$\varphi_{2,8}(x, t) = -\frac{2\sqrt{3}}{\sqrt{-\alpha(\beta f^2 + 1)}\left(\frac{x^\gamma}{\gamma} - \frac{bt^\delta}{\delta}\right)} + \frac{n^2v\left(\frac{x^\gamma}{\gamma} - \frac{bt^\delta}{\delta}\right)}{\sqrt{3}\sqrt{-\alpha(\beta f^2 + 1)}}. \quad (41)$$

Case-3

If $\mu > 0$, we obtain

$$\varphi_{2,9}(x, t) = -\frac{2\sqrt{3}nv \coth\left(\frac{\sqrt{\mu}n\left(\frac{x^\gamma}{\gamma} - \frac{bt^\delta}{\delta}\right)}{\sqrt{6}}\right)}{\sqrt{\mu}\sqrt{-\alpha(\beta f^2 + 1)}} - \frac{\sqrt{\mu}n \tanh\left(\frac{\sqrt{\mu}n\left(\frac{x^\gamma}{\gamma} - \frac{bt^\delta}{\delta}\right)}{\sqrt{6}}\right)}{\sqrt{3}\sqrt{-\alpha(\beta f^2 + 1)}}, \quad (42)$$

or

$$\varphi_{2,10}(x, t) = -\frac{2\sqrt{3}nv \tanh\left(\frac{\sqrt{\mu}n\left(\frac{x^\gamma}{\gamma} - \frac{bt^\delta}{\delta}\right)}{\sqrt{6}}\right)}{\sqrt{\mu}\sqrt{-\alpha(\beta f^2 + 1)}} - \frac{\sqrt{\mu}n \coth\left(\frac{\sqrt{\mu}n\left(\frac{x^\gamma}{\gamma} - \frac{bt^\delta}{\delta}\right)}{\sqrt{6}}\right)}{\sqrt{3}\sqrt{-\alpha(\beta f^2 + 1)}}. \quad (43)$$

4. Results and Discussions

This section demonstrates the uniqueness and importance of our research by meticulously comparing our obtained results with previously established findings. Notably, Tang and Chen introduced the complete linear discriminate scheme method for classifying single traveling wave solutions, while Wang and Wang utilized the fractional-order Riccati approach and the fractional-order dual-function method. In this study, we extend these methodologies by employing the SSRT and IGTHT. A detailed scrutiny of these prior investigations underscores the uniqueness of our results, which have not been documented in the previous literature. These novel findings, distinctly labeled, represent significant contributions to the field. Furthermore, we posit that our derived solutions offer valuable insights for understanding various physical phenomena.

The graphical representations provided in Figures 1–14 offer a comprehensive overview of the diverse types of solutions derived from the equations detailed in the text. We verify that all obtained soliton solutions satisfy Equation (1). Figure 1 illustrates the bright soliton solution derived from Equation (15), showcasing the localized, coherent wave packets characteristic of bright solitons. Figures 2 and 3 depict bright periodic singular soliton and bright singular solutions, respectively, each derived from Equations (16), (23) and (24), and Equation (17). Figure 4 presents a series of singular bell-shaped soliton solutions, exhibiting the characteristic bell-shaped profiles with singular features, obtained from Equations (18), (20), (22), (25), (27), and (28). Moving to Figures 5–7, dark soliton, singular bell-shaped periodic soliton, and dark periodic singular soliton solutions are displayed, each capturing distinct features of Equations (19), (21), and (26), respectively.

Figures 8–12 delve into solitary wave solutions, with Figure 8 showcasing periodic kink solitary waves from Equations (33) and (41), and Figure 9 depicting the combination of singular kink periodic solitary wave solutions derived from Equations (34) and (42). Additionally, Figures 10–12 present dark kink singular solitary wave, singular kink fusion solitary waves, and kink singular solitary wave solutions, respectively, each exhibiting unique characteristics, as dictated by their corresponding equations. Finally, Figures 13 and 14 provide visual representations of singular kink fusion solitary wave solutions obtained from Equations (42) and (43), further enriching the understanding of the complex dynamics and interactions present in the studied nonlinear system. These detailed graphical representations serve as valuable tools for elucidating the behavior and properties of the derived solutions, offering insights into the rich and varied dynamics of the nonlinear fractional-order Schrödinger model under investigation.

The graphical representations provided in Figures 1–14 offer a comprehensive overview of the diverse types of solutions derived from the equations detailed in the text. We categorize these solutions into distinct classes based on their characteristics:

- **Bright Soliton Solutions:**
 - Figure 1: Bright soliton solution derived from Equation (15), showcasing localized, coherent wave packets characteristic of bright solitons.
- **Bright Periodic Singular Soliton Solutions:**
 - Figure 2: Bright periodic singular soliton solution derived from Equations (16) and (23).
 - Figure 3: Bright singular solution derived from Equations (24) and (17).
- **Singular Bell-Shaped Soliton Solutions:**
 - Figure 4: Series of singular bell-shaped soliton solutions obtained from Equations (18), (20), (22), (25), (27), and (28).
- **Dark Soliton Solutions:**
 - Figure 5: Dark soliton solution derived from Equation (19).
- **Dark Periodic Singular Soliton Solutions:**
 - Figure 6: Singular bell-shaped periodic soliton solution obtained from Equation (21).
 - Figure 7: Dark periodic singular soliton solution derived from Equation (26).
- **Solitary Wave Solutions:**
 - Figure 8: Periodic kink solitary wave solution derived from Equations (33) and (41).
 - Figure 9: Combination of singular kink periodic solitary wave solutions obtained from Equations (34) and (42).
 - Figures 10–12: Dark kink singular solitary wave, singular kink fusion solitary waves, and kink singular solitary wave solutions, each exhibiting unique characteristics, as dictated by their corresponding equations.
- **Singular Kink Fusion Solitary Wave Solutions:**
 - Figures 13 and 14: Singular kink fusion solitary wave solutions obtained from Equations (42) and (43).

These detailed classifications and labels serve to clearly distinguish the various types of soliton solutions presented in the graphical representations, facilitating a better understanding of their characteristics and implications in the studied nonlinear fractional-order Schrödinger model.

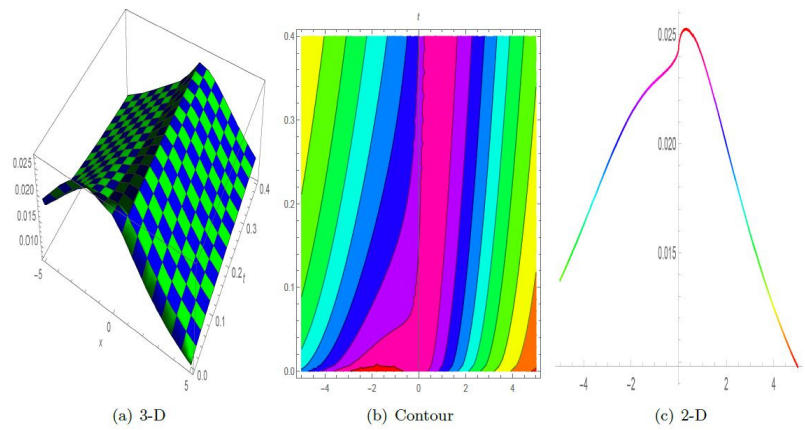


Figure 1. The bright soliton solution of (15), where $a = 2.4, \alpha = 0.1, m = 0.5, g = 0.4, \beta = 3.1, b = 1.4, \gamma = -1.7, f = 0.2, \delta = 0.5$ and $n = 1$.

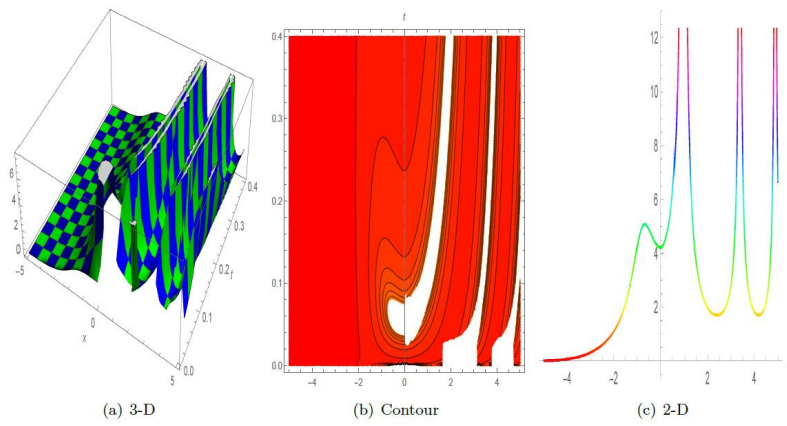


Figure 2. The bright periodic singular soliton solution of (16), where $\alpha = 0.1, m = 0.5, \beta = 3.1, b = 1.4, \gamma = -1.7, f = 0.2, \delta = 0.5, n = 1$ and $h = -0.3$.

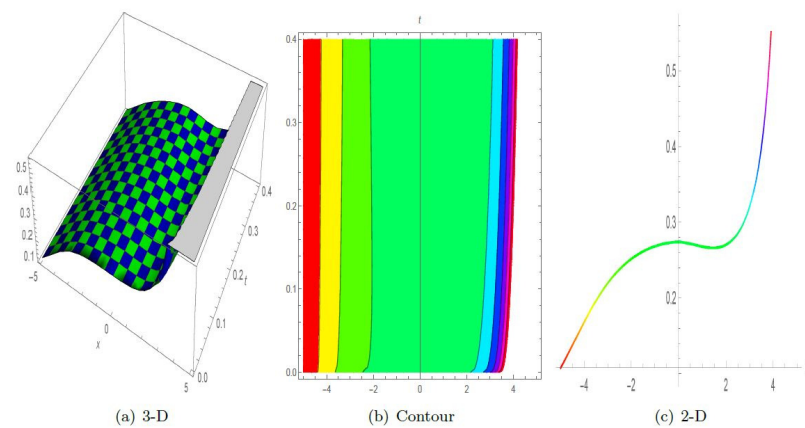


Figure 3. The bright singular solution of (17), where $\alpha = 0.1, m = 0.5, \beta = 3.1, b = 1.4, \gamma = -1.7, f = 0.2, \delta = 0.5, n = 1$ and $h = -0.3$.

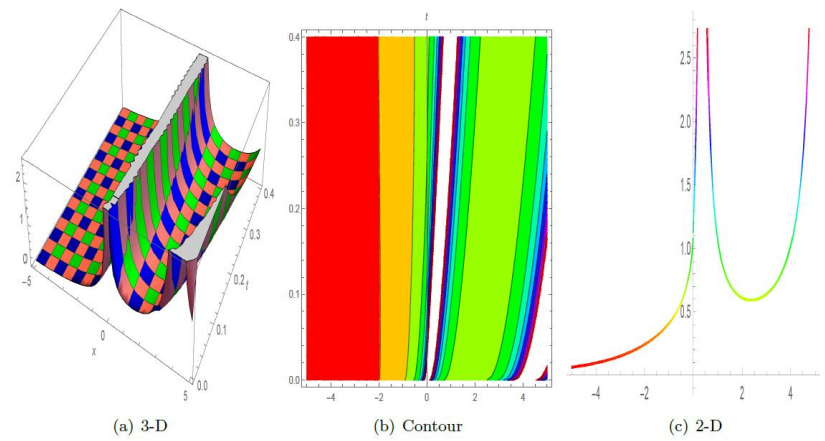


Figure 4. The singular bell-shaped soliton solution of (18), where $\alpha = 0.1, m = 0.5, \beta = 3.1, b = 1.4, \gamma = -1.7, f = 0.2, \delta = 0.5, n = 1$ and $h = -0.3$.

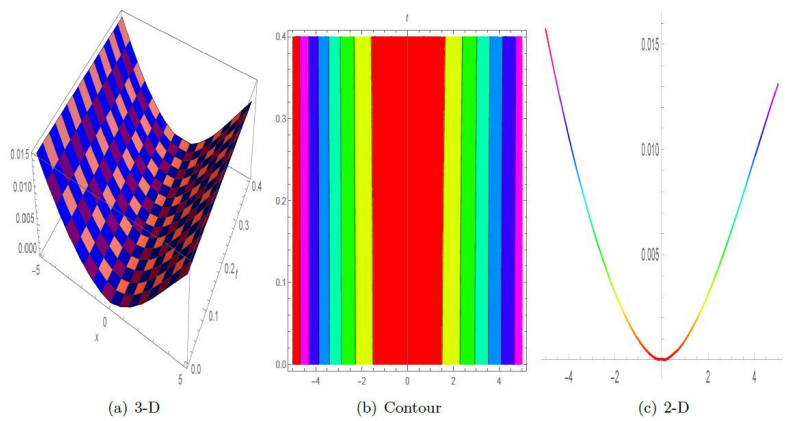


Figure 5. The dark soliton solution of (19), where $\alpha = 0.1, m = 0.5, \beta = 3.1, b = 1.4, \gamma = -1.7, f = 0.2, \delta = 0.5, n = 1$ and $h = -0.3$.

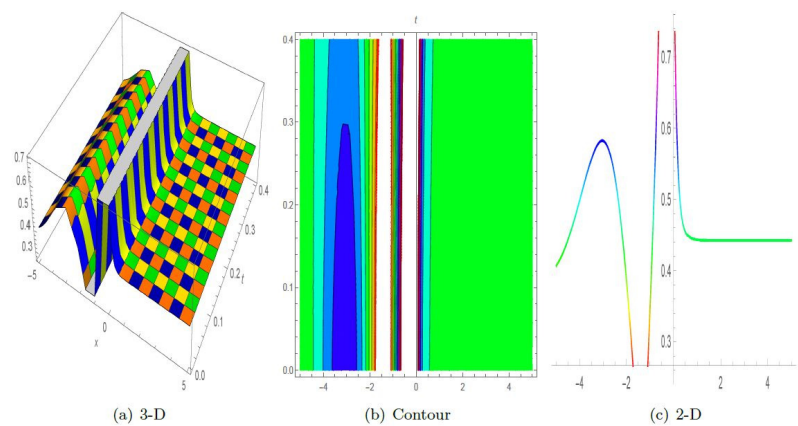


Figure 6. The singular bell-shaped periodic soliton solution of (21), where $\alpha = 0.1, m = 0.5, \beta = 3.1, b = 1.4, \gamma = -1.7, f = 0.2, \delta = 0.5, n = 1$ and $h = -0.3$.

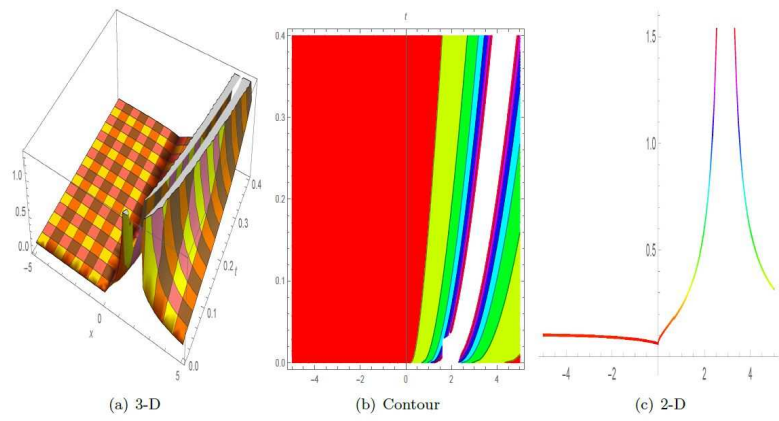


Figure 7. The dark periodic singular soliton solution of (26), where $\alpha = 0.1, m = 0.5, \beta = 3.1, b = 1.4, \gamma = -1.7, f = 0.2, \delta = 0.5, n = 1$ and $h = -0.3$.

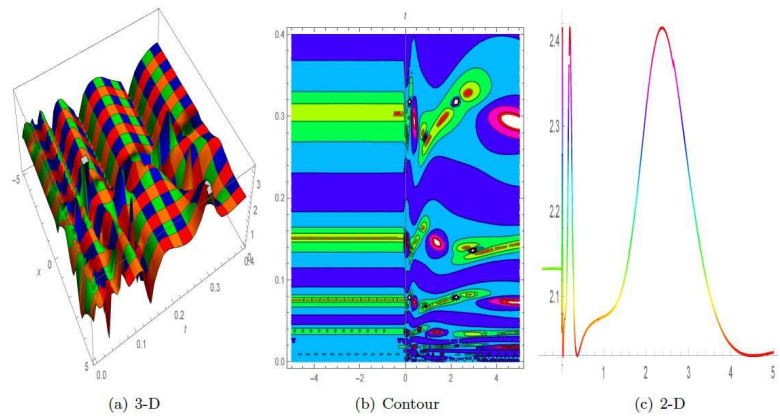


Figure 8. The periodic kink solitary waves solutions of (33), where $\alpha = 0.1, m = 0.5, \beta = 3.1, b = 1.4, \gamma = -1.7, f = 0.2, \delta = 0.5$ and $n = 1$.

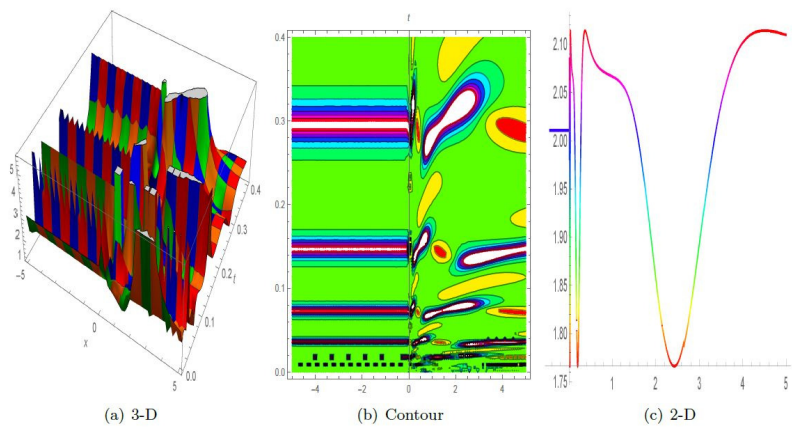


Figure 9. The combo of singular kink periodic solitary wave solutions of (34), where $\alpha = 0.1, m = 0.5, \beta = 3.1, b = 1.4, \gamma = -1.7, f = 0.2, \delta = 0.5$ and $n = 1$.

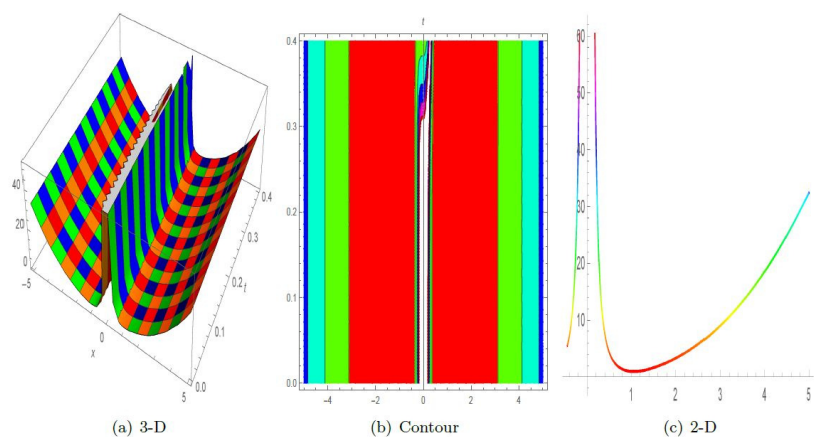


Figure 10. The dark kink singular solitary wave solution of (35), where $\alpha = 0.1, m = 0.5, g = 0.4, \beta = 3.1, b = 1.4, \gamma = -1.7, f = 0.2, \delta = 0.5$ and $n = 1$.

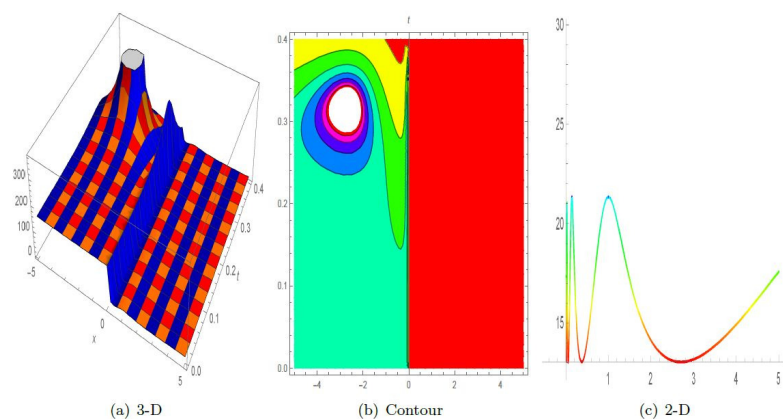


Figure 11. The singular kink fusion solitary waves solution of (37), where $\alpha = 0.1, m = 0.5, \beta = 3.1, b = 1.4, \gamma = -1.7, f = 0.2, \delta = 0.5$ and $n = 1$.

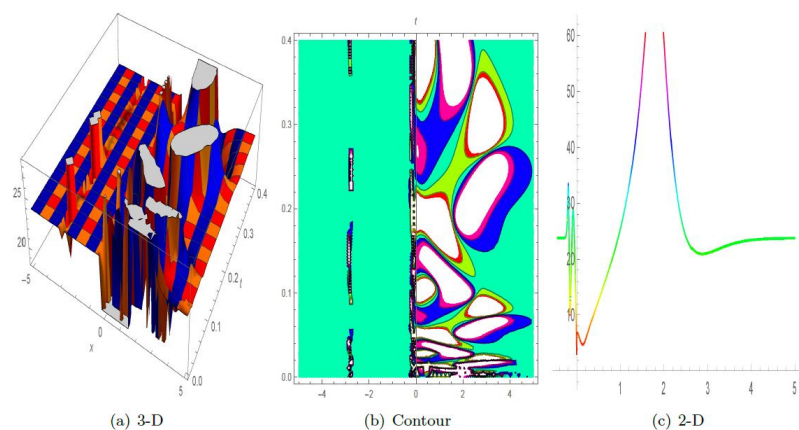


Figure 12. The kink singular solitary wave solution of (39), where $\alpha = 0.1, m = 0.5, \beta = 3.1, b = 1.4, \gamma = -1.7, f = 0.2, \delta = 0.5$ and $n = 1$.

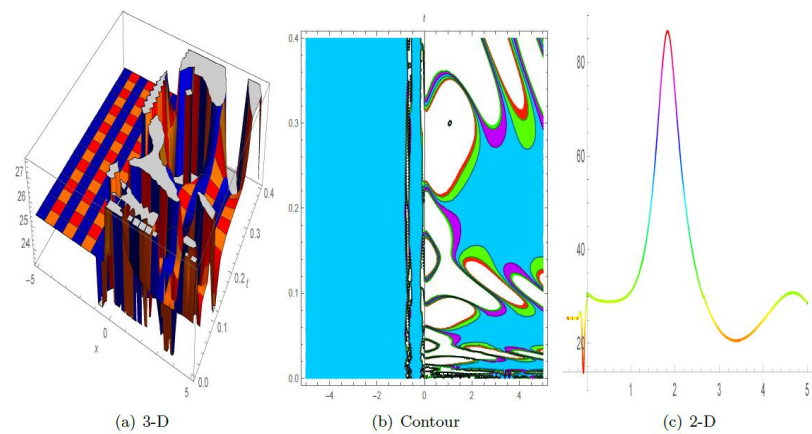


Figure 13. The singular kink fusion solitary waves solution of (42), where $\alpha = 0.1, m = 0.5, \beta = 3.1, b = 1.4, \gamma = -1.7, f = 0.2, \delta = 0.5$ and $n = 1$.

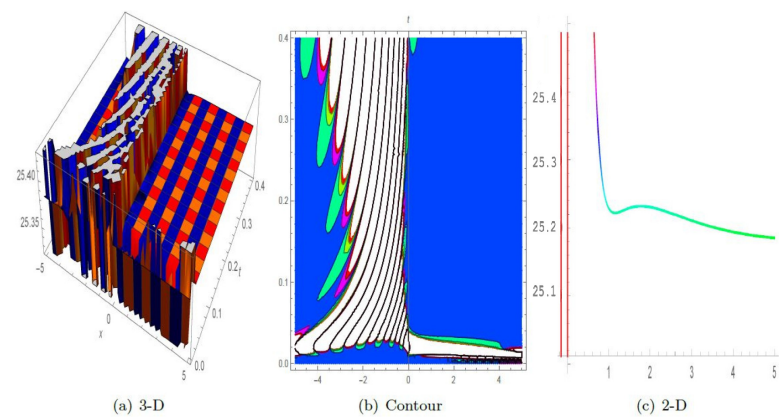


Figure 14. The singular kink fusion solitary waves solution of (43), where $\alpha = 0.1, m = 0.5, \beta = 3.1, b = 1.4, \gamma = -1.7, f = 0.2, \delta = 0.5$ and $n = 1$.

5. Conclusions

In conclusion, the fractional-order nonlinear Schrödinger model serves as an example of a globally recognized nonlinear model that accommodates various physiological nonlinearities. Utilizing two efficient techniques, the improved generalized tanh-function method (IGTHFM), and the Sardar-subequation method (SSEM), a diverse array of cases has been examined. Observations include bell-shaped, dark singular, periodic singular, and combination singular bright solitons. Additionally, periodic solitary waves, singular periodic, multi-waves, and combinations of multi-kink singular solitary wave solutions have been identified, broadening the scope of known solutions. To enhance understanding, graphical representations elucidating the dynamical behavior of dominant models characterizing pulse interaction concerning soliton variables have been provided. These solution sets exhibit reliability and productivity, showcasing the effectiveness of the employed methods. Furthermore, these calculated data hold the potential to expedite the evaluation and enhancement of optical fiber wave solution efficiency. In summary, the findings contribute to advancing the understanding of nonlinear phenomena, offering valuable insights into the behavior of fractional-order nonlinear Schrödinger models and guiding future research efforts in this domain.

Author Contributions: Conceptualization, R.P.A.; Data curation, A.K.; Funding acquisition, P.O.M. and R.P.A.; Investigation, R.P.A. and M.A.; Methodology, I.B.; Resources, M.A.Y.; Software, M.A.; Supervision, I.B.; Validation, P.O.M. and M.A.Y.; Visualization, A.K.; Writing—original draft, P.O.M., I.B. and M.A.Y.; Writing—review and editing, A.K. All authors have read and agreed to the published version of the manuscript.

Funding: Researchers Supporting Project number (RSP2024R136), King Saud University, Riyadh, Saudi Arabia.

Data Availability Statement: Data are contained within the article.

Acknowledgments: Researchers Supporting Project number (RSP2024R136), King Saud University, Riyadh, Saudi Arabia.

Conflicts of Interest: The authors declare that they have no competing interests.

References

- Zulfiqar, A.; Ahmad, J. Soliton solutions of fractional modified unstable Schrödinger equation using Exp-function method. *Results Phys.* **2020**, *19*, 103476.
- Fatima, M.; Agarwal, R.P.; Abbas, M.; Mohammed, P.O.; Shafiq, M.; Chorfi, N. Extension of Cubic B-Spline for Solving the Time-Fractional Allen–Cahn Equation in the Context of Mathematical Physics. *Computation* **2024**, *12*, 51.
- Ehsan, H.; Abbas, M.; Nazir, T.; Mohammed, P.O.; Chorfi, N.; Baleanu, D. Efficient analytical algorithms to study Fokas dynamical models involving M-truncated derivative. *Qual. Theory Dyn. Syst.* **2024**, *23*, 49.
- Yousaf, M.Z.; Srivastava, H.M.; Abbas, M.; Nazir, T.; Mohammed, P.O.; Vivas-Cortez, M.; Chorfi, N. A Novel Quintic B-Spline Technique for Numerical Solutions of the Fourth-Order Singular Singularly-Perturbed Problems. *Symmetry* **2023**, *15*, 1929.
- Wang, K.J. Variational principle and diverse wave structures of the modified Benjamin–Bona–Mahony equation arising in the optical illusions field. *Axioms* **2022**, *11*, 445.
- Zulfiqar, A.; Ahmad, J.; Ul-Hassan, Q.M. Analysis of some new wave solutions of fractional order generalized Pochhammer–chree equation using exp-function method. *Opt. Quantum Electron.* **2022**, *54*, 735.
- Islam, S.R.; Arafat, S.Y.; Wang, H. Abundant closed-form wave solutions to the simplified modified Camassa–Holm equation. *J. Ocean Eng. Sci.* **2022**, *8*, 238–245.
- Shakeel, M.; El-Zahar, E.R.; Shah, N.A.; Chung, J.D. Generalized Exp-Function Method to Find Closed Form Solutions of Nonlinear Dispersive Modified Benjamin–Bona–Mahony Equation Defined by Seismic Sea Waves. *Mathematics* **2022**, *10*, 1026.
- Joseph, S.P. Exact Traveling Wave Doubly Periodic Solutions for Generalized Double Sine-Gordon Equation. *Int. J. Appl. Comput. Math.* **2022**, *8*, 42.
- Athron, P.; Fowlie, A.; Lu, C.T.; Wu, L.; Wu, Y.; Zhu, B. Hadronic Uncertainties versus New Physics for the W boson Mass and Muon $g - 2$ Anomalies. *Nat. Commun.* **2023**, *14*, 659.
- Seidel, A. Integral Approach for Hybrid Manufacturing of Large Structural Titanium Space Components. Ph.D. Thesis, Dresden University of Technology, Dresden, Germany, 2022.
- Saifullah, S.; Ahmad, S.; Alyami, M.A.; Inc, M. Analysis of interaction of lump solutions with kink-soliton solutions of the generalized perturbed KdV equation using Hirota-bilinear approach. *Phys. Lett. A* **2022**, *454*, 128503.
- Liu, S.Z.; Wang, J.; Zhang, D.J. The Fokas–Lenells equations: Bilinear approach. *Stud. Appl. Math.* **2022**, *148*, 651–688.
- Khater, M.M. Prorogation of waves in shallow water through unidirectional Dullin–Gottwald–Holm model; computational simulations. *Int. J. Mod. Phys. B* **2022**, *37*, 2350071.
- Muniyappan, A.; Sahasraari, L.N.; Anitha, S.; Ilakiya, S.; Biswas, A.; Yıldırım, Y.; Triki, H.; Alshehri, H.M.; Belic, M.R. Family of optical solitons for perturbed Fokas–Lenells equation. *Optik* **2022**, *249*, 168224.
- Zhang, T.; Li, M.; Chen, J.; Wang, Y.; Miao, L.; Lu, Y.; He, Y. Multi-component ZnO alloys: Bandgap engineering, hetero-structures, and optoelectronic devices. *Mater. Sci. Eng. R Rep.* **2022**, *147*, 100661.
- Mahmood, A.; Srivastava, H.M.; Abbas, M.; Abdullah, F.A.; Mohammed, P.O.; Baleanu, D.; Chorfi, N. Optical soliton solutions of the coupled Radhakrishnan–Kundu–Lakshmanan equation by using the extended direct algebraic approach. *Heliyon* **2023**, *9*, e20852.
- Min, R.; Hu, X.; Pereira, L.; Soares, M.S.; Silva, L.C.; Wang, G.; Martins, L.; Qu, H.; Antunes, P.; Marques, C.; Li, X. Polymer optical fiber for monitoring human physiological and body function: A comprehensive review on mechanisms, materials, and applications. *Opt. Laser Technol.* **2022**, *147*, 107626.
- Lechelon, M.; Meriguet, Y.; Gori, M.; Ruffenach, S.; Nardecchia, I.; Floriani, E.; Coquillat, D.; Teppe, F.; Mailfert, S.; Marguet, D.; Ferrier, P. Experimental evidence for long-distance electrodynamic intermolecular forces. *Sci. Adv.* **2022**, *8*, eabl5855.
- Tarla, S.; Ali, K.K.; Yilmazer, R.; Yusuf, A. Investigation of the dynamical behavior of the Hirota–Maccari system in single-mode fibers. *Opt. Quan. Electron* **2022**, *54*, 613.
- Ahmad, J. Dispersive multiple lump solutions and soliton’s interaction to the nonlinear dynamical model and its stability analysis. *Eur. Phys. J. D* **2022**, *76*, 14.
- Dubey, S.; Chakraverty, S. Application of modified extended tanh method in solving fractional order coupled wave equations. *Math. Comput. Simul.* **2022**, *198*, 509–520.

23. Siddique, I.; Mehdi, K.B.; Jarad, F.; Elbrolosy, M.E.; Elmandouh, A.A. Novel precise solutions and bifurcation of traveling wave solutions for the nonlinear fractional (3+ 1)-dimensional WBBM equation. *Int. J. Mod. Phys. B* **2022**, *37*, 2350011.
24. Ansar, R.; Abbas, M.; Mohammed, P.O.; Al-Sarairah, E.; Gepreel, K.A.; Soliman, M.S. Dynamical Study of Coupled Riemann Wave Equation Involving Conformable, Beta, and M-Truncated Derivatives via Two Efficient Analytical Methods. *Symmetry* **2023**, *15*, 1293.
25. Jiang, Y.; Wang, F.; Salama, S.A.; Botmart, T.; Khater, M.M. Computational investigation on a nonlinear dispersion model with the weak non-local nonlinearity in quantum mechanics. *Results Phys.* **2022**, *38*, 105583.
26. Bilal, M.; Rehman, S.U.; Ahmad, J. The study of new optical soliton solutions to the time-space fractional nonlinear dynamical model with novel mechanisms. *J. Ocean Eng. Sci.* **2022**. <https://doi.org/10.1016/j.joes.2022.05.027>.
27. Jan, A.; Srivastava, H.M.; Khan, A.; Mohammed, P.O.; Jan, R.; Hamed, Y.S. In Vivo HIV Dynamics, Modeling the Interaction of HIV and Immune System via Non-Integer Derivatives. *Fractal Fract.* **2023**, *7*, 361.
28. Chen, W.; Sun, H.; Li, X. *Fractional Derivative Modeling in Mechanics and Engineering*; Springer: Beijing, China, 2022.
29. Abouelregal, A.E.; Fahmy, M.A. Generalized Moore-Gibson-Thompson thermoelastic fractional derivative model without singular kernels for an infinite orthotropic thermoelastic body with temperature-dependent properties. *ZAMM-Z. Angew. Math. Mech.* **2022**, *102*, e202100533.
30. Zhu, Y.; Tang, T.; Zhao, S.; Joralmon, D.; Poit, Z.; Ahire, B.; Keshav, S.; Raje, A.R.; Blair, J.; Zhang, Z.; Li, X. Recent Advancements and Applications in 3D Printing of Functional Optics. *Addit. Manuf.* **2022**, *52*, 102682.
31. Li, Q.; Shan, W.; Wang, P.; Cui, H. Breather, lump and N-soliton wave solutions of the (2+ 1)-dimensional coupled nonlinear partial differential equation with variable coefficients. *Commun. Nonlinear Sci. Numer. Simul.* **2022**, *106*, 106098.
32. Bilal, M.; Ahmad, J. A variety of exact optical soliton solutions to the generalized (2+ 1)-dimensional dynamical conformable fractional Schrödinger model. *Results Phys.* **2022**, *33*, 105198.
33. Aniq, A.; Ahmad, J. Soliton solution of fractional Sharma-Tasso-Olevers equation via an efficient (G/G)-expansion method. *Ain Shams Eng. J.* **2022**, *13*, 101528.
34. Wang, K.J.; Liu, J.H.; Wu, J. Soliton solutions to the Fokas system arising in monomode optical fibers. *Optik* **2022**, *251*, 168319.
35. Mohammed, P.O. Some positive results for exponential-kernel difference operators of Riemann-Liouville type. *Math. Model. Control.* **2024**, *4*, 133–140.
36. Rezazadeh, H.; Sabu, J.; Zabihi, A.; Ansari, R.; Tunc, C. Implementation of soliton solutions for generalized nonlinear Schrödinger equation with variable coefficients. *Nonlinear Stud.* **2022**, *29*, 547–559.
37. Li, J.; Li, B. Mix-training physics-informed neural networks for the rogue waves of nonlinear Schrödinger equation. *Chaos Solit. Fractals* **2022**, *164*, 112712.
38. Chen, Y.; Li, B. N-soliton solutions for the novel Kundu-nonlinear Schrödinger equation and Riemann–Hilbert approach. *Wave Motion* **2024**, *127*, 103293.
39. Tang, X.S.; Li, B. Optical solitons and stability analysis for the generalized fourth-order nonlinear Schrödinger equation. *Mod. Phys. Lett. B* **2019**, *33*, 1950333.
40. Rezazadeh, H.; Inc, M.; Baleanu, D. New Solitary Wave Solutions for Variants of (3+1)-Dimensional Wazwaz-Benjamin-Bona-Mahony Equations. *Front. Phys.* **2020**, *8*, 332.
41. Ahmad, S.; Mahmoud, E.E.; Saifullah, S.; Ullah, A.; Ahmad, S.; Akgül, A.; El Din, S.M. New waves solutions of a nonlinear Landau–Ginzburg–Higgs equation: The Sardar-subequation and energy balance approaches. *Results Phys.* **2023**, *51*, 106736.
42. Ullah, N.; Asjad, M.I.; Awrejcewicz, J.; Muhammad, T.; Baleanu, D. On soliton solutions of fractional-order nonlinear model appears in physical sciences. *AIMS Math.* **2022**, *7*, 7421–7440.
43. Alsharidi, A.K.; Bekir, A. Discovery of New Exact Wave Solutions to the M-Fractional Complex Three Coupled Maccari’s System by Sardar Sub-Equation Scheme. *Symmetry* **2023**, *15*, 1567.
44. Tang, L. Exact solutions to conformable time-fractional Klein–Gordon equation with high-order nonlinearities. *Results Phys.* **2020**, *18*, 103289.
45. Zaman, U.H.M.; Arefin, M.A.; Akbar, M.A.; Uddin, M.H. Utilizing the extended tanh-function technique to scrutinize fractional order nonlinear partial differential equations. *Partial Differ. Equ. Appl. Math.* **2023**, *8*, 100563.
46. Mamun, A.A.; Ananna, S.N.; An, T.; Shahen, N.H.M.; Asaduzzaman, M.; Foyjonnesa. Dynamical behaviour of travelling wave solutions to the conformable time-fractional modified Liouville and mRLW equations in water wave mechanics. *Heliyon* **2021**, *7*, e07704.
47. Mamun, A.A.; Ananna, S.N.; Gharami, P.P.; An, T.; Asaduzzaman, M. The improved modified extended tanh-function method to develop the exact travelling wave solutions of a family of 3D fractional WBBM equations. *Results Phys.* **2022**, *41*, 105969.
48. Sadiya, U.; Inc, M.; Arefin, M.A.; Uddin, M.H. Consistent travelling waves solutions to the non-linear time fractional Klein–Gordon and Sine-Gordon equations through extended tanh-function approach. *J. Taibah Univ. Sci.* **2022**, *16*, 594–607.
49. Khalil, R.; Al Horani, M.; Yousef, A.; Sababheh, M. A new definition of fractional derivative. *J. Comput. Appl. Math.* **2014**, *264*, 65–70.

Disclaimer/Publisher’s Note: The statements, opinions and data contained in all publications are solely those of the individual author(s) and contributor(s) and not of MDPI and/or the editor(s). MDPI and/or the editor(s) disclaim responsibility for any injury to people or property resulting from any ideas, methods, instructions or products referred to in the content.